Enhanced Characterization of Depolarizing Samples Using Indices of Polarization Purity and Polarizance-Reflection-Transformation: Supplement material

Dekui Li [a,†], Ivan Monte[b,†], Mónica Canabal [b], Irene Estévez [b], Octavi Lopez-Coronado [b], Zhongyi Guo [a,*], Juan Campos [b], Angel Lizana [b,*]

[a]*School of Computer and information, Hefei University of Technology, Hefei 230009, China*
[b]*Optics Group, Departamento of Physics, Autonomous University of Barcelona, Bellaterra 08193, Spain*

1 Characterization of diattenuator-based depolarizers with different structural characteristics.

The corresponding distribution results in Figs. 4(a) and (b) in the main paper respectively demonstrate the certain ability of PRT and IPP spaces to distinguish between the depolarizers with the same origin but different inherent structural characteristics, since the IPP and PRT spaces are able to represent all depolarization systems, and furthermore each position in such spaces represents the case with unique polarization characteristics. In particular, in IPP space shown in Fig. 4(b) in the main paper, the distance between lines with σ^2 smaller than 0.15π is significant, but as σ^2 increases, the related representation lines keep approaching the limitation that the lines are almost totally coincident when the values of σ^2 are bigger than 0.25π. Conversely, the PRT space shows a good performance in distinguishing between lines representing depolarizers with different σ^2. In particular, the related lines have significant discrepancies, especially when σ^2 is smaller than 0.35π (it is a common range in biological tissues), which demonstrates the ability of PRT space to identify different diattenuator-based depolarizers.

Comparing cures with different controlling parameters, we realize that with the increase of σ^2, the corresponding cures get close to the plane (P_P=0) in PRT space. Note that the units within are polarization-anisotropy diattenuator with different diattenuation directions. As σ^2 continually increases, the directions of units become more diversified, which decreases the overall (microscopical) diattenuation for the consisted depolarizer. For this reason, the curves get close to the plane P_P=0. Moreover, the polarimetric observable P_P can form a function of the direction diversity characterized by σ^2, being an indicator useful to characteristic the direction diversity of units in the depolarizer. In addition, the increase of σ^2 results in more strong depolarization effect, leading that the corresponding curve approximate line P_1=P_2. In this vein, there is the other limitation where the σ^2 equals 0. In this case, the units are placed with the same direction, which means the depolarizer will show stronger diattenuation (corresponding to a big value of P_P), this leading to the case to be pure systems. As stated before, all pure systems are represented in the point (P_1=1, P_2=1, P_3=1) in IPP space. Conversely, in PRT space, the area representing pure systems is much bigger than a point. In particular, in PRT space, according to Eq. 11, the cure formed by all polarization pure systems is on the surface of $2P_P^2/3+R^2+T^2=1$, and the represented points moves with varying diattenuation.

In addition to the curve and points in the PRT and IPP space, representing the pure systems corresponding to σ^2 of 0, we next focus on an arbitrary curve in such two spaces to analyze more general mechanism. For instance, in IPP space decreasing D leads to nearness of point (P_1=1, P_2=1, P_3=1) which represents the pure system, and furthermore, as the limitation where D equals 0, the representing point approach the position (P_1=1, P_2=1, P_3=1). The polarimetric observable D characters the diattenuation of units within diattenuator-based depolarizers, and thus, if its units entirely lose diattenuation, the depolarizer is bound to degrade into an polarization-isotropy media without any kind of polarization effects, independently of the amplitude of randomness of unit directions. Therefore, whereas the value of σ^2 equaling 0, illustrating the definiteness of direction of units distributed in depolarizes, represents pure systems categorized as pure diattenuator, the D being 0, representing the fact that the related depolarizer loses all diattenuation, implies the pure system without any polarization effect. Analogously, in PRT space, with the decrease of D, the representing point gets closer to the position (P_P=0, R=1, T=0), representing polarization-isotropy pure systems.

In summary, both such polarization spaces are certainly capable of characterizing the diattenuator-based depolarizers with different structural characteristics, and moreover, PRT space shows significant superiorities over IPP space in several tasks. On one hand, whereas all diattenuator-based depolarizers fall on a fixed plane (P_3=1) in IPP space, PRT space illustrates a 3D distribution with a big volume of all diattenuator-based depolarizers, which leads that representing points of such depolarizers have bigger geometrical distance and less overlap in PRT space. On the other hand, unlike IPP space only containing the amplitude of randomness, the observables in PRT space have physical meaning, leading that PRT space performs better in analyzing diattenuator-based depolarizers. In particular, whereas IPP space cannot distinguish pure systems with different structures, PRT space can identify the structure of pure systems. With the consideration of the superiority of PRT space in characterizing depolarizers, in the main paper, the PRT space-related polarimetric observables are chosen to calculate the microscopic parameters of the depolarizers, forming Eqs. (13)-(16). It is worth noting here that Eqs. (13)-(16) may not be implemented on some complex scenarios, but we could construct, by means of an equivalent process to that leading to Eqs. (13)-(16) of the main paper, a new empirical function correlating microscopic parameters with macroscopic measurements, in this case, values in the PRT space

2 Characterization of retarder-based depolarizers with different structural characteristics.

we next study the suitability of the IPP and PRT associated polarimetric observables to characterize depolarizers originated by the incoherent addition of linear retarders, i.e., retarder-based depolarizers. As shown in Fig.5 in the main paper, due to the physical characteristics of the retarder-based depolarizers with varying controlling parameters, there are 10 cures with different colors representing related ϕ in each space, which present unique distributions and varying tendencies, in the studied spaces (P_1P_2 and RT spaces). In particular, unlike the diattenuator-based depolarizers whose position (or distribution) continually monotonic removes in PRT space with the varying parameters, the curves of retarder-based depolarizers in RP space start to go back when the ϕ is about bigger than 0.6π, and reoccupy the positions that have already been occupied by other retarder-based depolarizers. It means that some points in PRT space (herein RP space) have ambiguity, in which one position does not relate to a fixed retarder-based depolarizer, causing that retarder-based depolarizers cannot be identified only according to their distribution position in RP space. In contrast, in P_1P_2 space, the result is under the expectation that as ϕ increases, the curves fill the physically achievable area continually with a limitation where the representing curves is coincident with the line P_2=1 when ϕ approaches π. The case of P_2=1 represents the depolarizers under study is so called 2D depolarizers that can be regarded as being consisted of two pure systems. Therefore, under this condition, IPP space performs better over PRT space since the IPP space effectively avoids the ambiguity of positions and provides a clear physical mean with varying parameters. However, there is still a problem about P_1P_2 space, in which, for instance, curves only share a limited area and thus the distance between cures is slight, causing it remains a challenge to identify retarder-based depolarizers. Fortunately, if we focus on the curve distributions when ϕ is bigger than 0.6 π (or ϕ is smaller than 0.6 π), the RT space shows a significant ability to identify retarder-based depolarizers.

To further confirm the above statement, the curves related to ϕ from 0.1π to 0.5π are represented in RP and P_1P_2 spaces (respectively see Fig. 5(c) and (d) main paper). The superiority of RP space over P_1P_2 can be apparently seen. On the one hand, all curves state from the point (1,1) representing pure systems in P_1P_2 space, which determines there are inevitable overlaps among curves in P_1P_2 space, especially when σ^2 is small. The reason is understandable because that the retarder-based depolarizer with slight σ^2 is closer to pure systems that lies on (1,1). Besides, in P_1P_2 space, the curve with bigger ϕ always higher than that with smaller ϕ, which demonstrates that the increase of ϕ leads the decrease of depolarization effect. On the other hand, in RT space, the samples of ϕ=0 are represented in the point (1, 0). It is reasonable since the samples with ϕ=0 do not have any polarization effect and thus their MM is diag(1, 0, 0, 0). As the value of ϕ increases from 0.1π to 0.5π, the corresponding curves far away from the point (1, 0), which result from the decreased corresponding polarimetric observable R with the increase of ϕ. In addition, the distances between curves representing different ϕ are much bigger than that in P_1P_2 space. More importantly, such curves are almost mutually parallel, and are all perpendicular to the R axis, resulting in the absence of overlap, this strongly demonstrating the ability of RT space to distinguish between retarder-based depolarizers over P_1P_2 space.

Comparing the results in P_1P_2 and RT spaces, they both possess relative advantages regarding retarder-based depolarizers identification. In particular, RT space does possess the ability to highlight the difference between studying depolarizers. However, there are some overlaps appearing when ϕ is bigger than about 0.6π. In contrast, this problem is perfectly resolved in P_1P_2 space, in which with the increase of ϕ the representing curves continually fill P_1P_2 space without appearing overlap. However, the small discrepancy between different retarder-based depolarizers geometrically represented by P_1P_2 space makes the retarder-based depolarizers almost unidentifiable, especially when the represented points get closer to the line P_2=1. For this reason, the method combining RP and P_1P_2 spaces is able to identify retarder-based depolarizers with a full possible range of ϕ in a perfect way. In particular, the representing point of the corresponding retarder-based depolarizer firstly is placed in P_1P_2 space to judge the relative position compared with the curve of ϕ =0.6π. For instance, if the point falls on the position lower than the curve of ϕ =0.6π, we then focus on the distribution in RT space shown in Fig. 5(c) in the main paper to calculate the controlling parameters. Otherwise, the other part is selected to obtain the controlling parameters in the same way.

3 Characterization of depolarizers originated by dispersion of the mean polarimetric values.

In this section, we study the depolarization resulting from the diattenuation and retardance dispersions. To do so, a series of depolarizers with fixed direction dispersion has been constructed. First, for the retarder-based depolarizers, each new retarder-based depolarizer is built from 300 retarders. Moreover, the dispersion of such retarders is assigned as obeying Gaussian distribution (the mean value of the axis position is π/3 and the variance is π/9). Under this scenario, the mean value and variance of retardance are changed to study the depolarization of the constructed retarder-based depolarizers. In particular, the mean value of retardance ranges from 0.1π to π radians with a step of 0.1π, and the variance ranging from 0 to π/8 is divided into 300 parts. Therefore, there are 3000 retarder-based depolarizers generalized to study depolarization in IPP and PRT spaces. New results are shown in following Fig. S1:

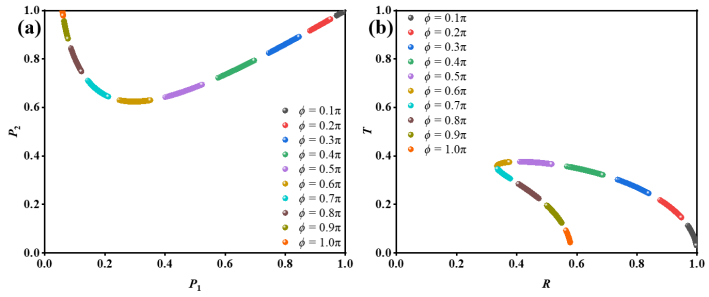

Fig. S1. Representation of the simulated retarder-based depolarizers with different dispersions with respect to the mean retarder value, represented in different depolarization spaces: (a) IPP space; and (b) PRT space.

Figure S1 illustrates the distributions with the retardance mean value and retardance variance, where the curves marked by different colors represent different retardance mean values and points on each curve represent a different variance value considered. As illustrated in IPP and PRT spaces, the retarder-based retarders occupy different curves (colors) with the change of retardance mean values. Importantly, each dispersion value selected provides a different point to a particular color curve (mean phase value). Therefore, the specific position of a point into a color curve in Fig. S1 states the dispersion of mean-retardance value selected, this demonstrating the capability of the spaces to discriminate mean phase dispersions values. To reinforce this idea, note that no color curve is overlapped in the spaces, both in the IPP (Fig. S1(a)) and PRT (Fig. S1(b)) spaces. Therefore, we demonstrate that both in IPPs and PRT spaces are suitable spaces to discriminate against retarder-based depolarizers originated by different retardance distributions.

As a complement to retarder-based depolarizers, diattenuator-based depolarizers are also studied to show the depolarization origin of diattenuation dispersion. To study this case, the diattenuation is further divided into two components, Px and Py. Px represents the attenuation of X direction, whereas Py represents the attenuation of Y direction. Here we follow the same procedure for diattenuation-based depolarizers with different mean diattenuation distributions, as in the previous retarder-based depolarizes case. In particular, we set all depolarizers to Px=1, and then, the dispersion value from the mean diattenuation value obeying a Gaussian distribution. As in the previous case, we selected an arbitrary orientation for diattenuators of $\pi/3$, and a fixed orientation dispersion of $\pi/9$ to generate depolarizers. After that, there are two available parameters (the mean value of Py and its variance) to adjust the diattenuator-based depolarizers. Herein, the Py ranges from 0.1 to 1 with the step of 0.1, the variance ranging from 0 to 1/8 is divided to 300 parts. By assigning the values of Py and variance, the 3000 diattenuator-based depolarizers are generalized, and the corresponding represented points in IPP and PRT spaces are illustrated in Figs. S2(a) and S2(b) of the new manuscript, respectively.

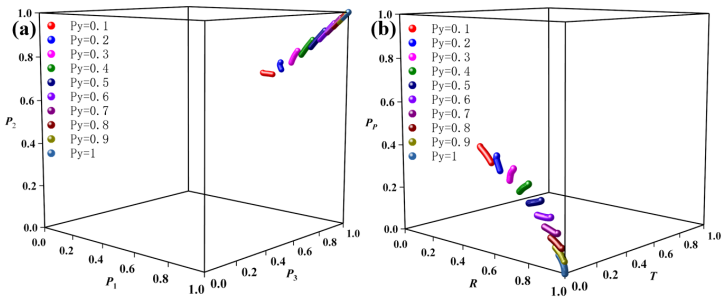

Fig. S2. Representation of the simulated diattenuator-based depolarizers with different Py mean values (Px=1) in different representation spaces: (a) IPP space; and (b) PRT space.

According to the calculation equation of diattenuation (D) shown in ref [5] in the main paper, the higher value of Py, the weaker diattenuation of diattenuators inside. As shown in IPP space (see Fig. S2(a)), the curves with high Py are close to the point (1,1,1) representing non-depolarization systems. Moreover, near this point, the curves with different Py are almost coincident. It makes it difficult to distinguish such depolarizers in IPP space because their depolarizing capability is too weak. Conversely, In PRT space, curves with different Py occupy different areas, leading corresponding depolarizes can be identified. These results provided that both spaces (Figs. S2(a) and (b)) have the potential to discriminate between different diattenuator mean values (different color curves) and different dispersion values for each particular diattenuator mean value (different points in a particular curve). Importantly, by comparing Figs. S2(a) and (b) we can also state that the PRT space is more adequate for this task, as better separates the different cases, occupying a larger volume.

Summarizing, the results in Figs. S1 and S2 demonstrate that the IPP space, and especially, the PRT space, are suitable to discriminate against the case of study proposed by the reviewer, i.e., discriminating scenarios of depolarizers originated by dispersion of the mean polarimetric values

4 Distinction between different depolarization origins in anisotropic depolarizers.

This section is devoted to the studying the retarder-diattenuator-based depolarizer that contains retarders and diattenuator at the same time. For the combination case, we construct an incoherent addition of the two pure cases (retardance based and diattenuation based depolarizers). We set a weight for each type of 50% (150 retarders and 150 diattenuators). As in previous cases, mean values (retardance and diattenuation), mean orientations, and dispersion of orientation (following a Gaussian distribution) are the control parameters. Herein, the mean orientation of such retarders and diattenuators inside is π/3, and the variance ranging from 0 to π/2 is divided into 300 parts. The retardance ranges from 0 to π/2 with 300 parts and diattenuation ranges from 0 to 1 with 300 parts. By assigning the variance of orientation and the pair of diattenuation and retardance, 90000 (300×300) retarder-diattenuator depolarizers are constructed. Corresponding results are given in blue both for the IPP (Fig. S3(a)) and PRT (Fig. S3(b)) spaces. For comparison, the pure cases of diattenuation-based depolarizers (in red) and retarder-based depolarizers (in green) already discussed in Fig. 3 of the main manuscript are also represented in Fig. S3.

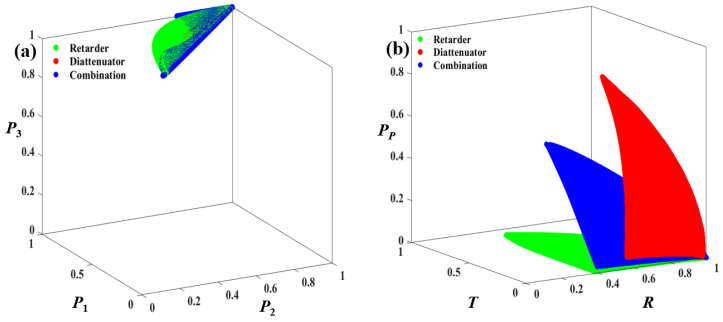

Fig. S3. The distributions of diattenuator-based (red color) depolarizers, retarder-based (green color) depolarizers and diattenuator-retarder-based depolarizers (blue color) represented in the studied depolarizing spaces: (a) The IPP space; (b) The PRT space

As shown in Fig. S3, in IPP space, all corresponding points are located on the surface P_3=1 (Note that the diattenuator-based depolarizers represented by red points are covered by other points), independently of the depolarization origins. This phenomenon is easy to understand since it has been demonstrated that all anisotropic depolarizers have P_3 of 1. For this reason, the IPP space cannot distinguish between different depolarization origins in anisotropic depolarizers. Conversely, the PRT space can distinguish between different depolarization origins, including mixtures of diattenuation and retardance-based depolarizers. In particular, as shown in Fig. S3(b), the retarder-diattenuator-based depolarizers (blue data) are located between retarder-based depolarizers (green data) and diattenuator-based depolarizers (red data), and there is only one coincident point (0,1,1) in PRT space, this corresponding to non-depolarizing systems. In addition, we see how the distance of the retarder-diattenuator-based depolarizers surface occupies an intermediate location between the pure cases. This situation is related to the selected 50% weighted. If other weighted values are considered, this surface moves closer to the corresponding pure system. This situation shows how the PRT space is especially sensible against different diattenuation-retarder-based depolarizers.